

Thermal performance assessment of a Parabolic Trough Collector prototype system in Palapye, Botswana

Ndakidzilo Nthoiwa

Department of Physics and Astronomy
BIUST
Palapye, Botswana
ndakidzilo.nthoiwa@studentmail.biust.ac.bw

Einax Mario

Department of Physics and Astronomy
BIUST
Palapye, Botswana
einaxm@biust.ac.bw

Abstract— A parabolic trough collector (PTC) prototype was fabricated and tested at Palapye (22.59404 °S and 027.12455 °E) in Botswana. A stainless steel sheet lined with an adhesive Mylar film of high reflectivity (≥ 0.94) was used as the collector with area 3.001 m² and a copper tube of 15 mm external diameter and length 2.440 m coated with silicone 250 selective coating as the receiver. The performance of the coated receiver tube was compared to that of a 2.0 m long commercial receiver without any modification of the collector. The highest outlet temperature of 75.8 °C was achieved, with inlet water and ambient temperatures of 26.1 and 28.0 °C, respectively. The effect of the wind speed, mass flow rate of the water and the irradiation on the thermal efficiencies of the system were studied. An increase in the average wind speed from 2.8 to 4.4 m/s resulted in both the Carnot and thermal efficiency decreasing from 61.1 to 54.1 % and 20.3 to 7.7 %, respectively. At constant wind speed, a decrease in the flow rate from 0.0036 to 0.0012 kg/s resulted in an increase in the Carnot efficiency from 43.9 to 54.1 % due to an increase in the outlet temperature, while the thermal efficiency dropped by half. The wind speed had no influence on the commercial receiver outlet temperature because of the vacuum insulation.

Keywords— Solar energy; Parabolic trough collector; Thermal efficiency; Carnot efficiency

I. INTRODUCTION

Parabolic trough collector (PTC) is the mostly adopted and mature of all the four concentrating solar power technologies (CSPT), constituting over 90 % of the total world installed concentrated solar power plants [1]. A PTC is made of three components; the receiver, collector and the support structure. A collector is a parabolic shaped sheet lined with a reflective material, which focuses all the irradiation falling on its surface to the focal line. A commercial receiver or a pipe coated with a solar selective paint is placed at the collector's focal line to absorb the heat and raise the temperature of the fluid passing through it. Nine solar power plants established between 1985 and 1991 and known as the solar energy generating systems (SEGS) in the Mojave desert, southern California with a combined power of 354 MWe are the pioneers of concentrated solar power (CSP). It remains the biggest commercial and combined operational plants which have adopted the use of parabolic trough collectors (PTCs) [2].

The idea of harnessing solar radiation using this technique was triggered by the surging oil prices around 1979 [3], but in 1990 the prices dropped, resulting in a break from the investment in solar thermal technologies up to the year 2000 [1]. An additional 780 MWe of CSP was added between 2007 and 2010, with over half being commissioned in 2010 alone hence increasing the global total to 1095 MWe. By 2015 the global total of installed CSP had increased to 4950 MWe from 4534 MWe the previous year [4]. Africa has also adopted the technology with countries such as South Africa, Morocco, Egypt and Algeria having operational plants ranging from 20 MWe to 160 MWe. By end of 2019, South Africa is expected to generate 700.1 MWe from its eight power plants, five of which adopted the PTC technology. Morocco has also set a very ambitious milestone of achieving 2 GW of solar renewables by 2020; 42 % of the country's energy mix [5]. On the contrary, Botswana is yet to construct the first CSP plant, with a projected capacity of 50 MWe in Jwaneng and Maun.

The daily irradiation in Botswana is enough to drive CSP stations to produce more than enough electricity to sustain the current 669 MW peak power demand. On average the country experiences over 320 clear sky days annually, receiving an average horizontal insolation of 21 MJ/m² per day on a flat surface. But surprisingly, Botswana is still reliant on coal powered Morupule B power station, the giant power producer in the country. Diesel generators of 70 MW and 105 MW at Orapa and Matshelegabedi respectively, have also been deployed to augment the projected power demand at a peak of 669 MW in winter [6]. Importation of power from neighboring South Africa and Mozambique on a firm and non-firm basis is also ongoing.

This paper reports on the performance of the first parabolic trough collector prototype system constructed locally and tested at a site in Palapye. This is the first prototype to be built and tested locally and it will serve as a source of information and proof of concept for scientists, entrepreneurs and the government when deciding whether or not to invest in solar thermal technologies either for industrial applications, water desalination, generation of steam for sterilization and even power generation.

II. METHODOLOGY

The PTC prototype shown in Fig. 1 was fabricated at a local metal workshop called “Supu Metal Clinic” with the help of a local craftsman using locally available materials.

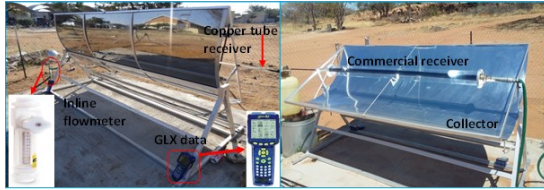


Fig. 1 The experimental set-up of the PTC with a copper tube receiver and the commercial receiver with a glass envelope.

A mirror finish-stainless steel was curved into a trough and held into the desired position with the support structures. A copper pipe of external was used as the receiver and it was drilled near both ends to insert Xplorer GLX temperature probes and the holes sealed with Pratley putty. The pipe was then coated with a selective solar paint (Thurmalox 250), which has low emissivity of 52 % and high absorptivity of 96 % in the solar spectrum range (wavelengths between 0.3 μm to 3.0 μm). The prototype was then mounted on a concrete slab, at geographical coordinates 22.59404 °S and 027.12455 °E and an altitude of 973 m. The specific dimensions and properties of the various characteristics of the prototype are given in Table 1.

Table 1 Key features of the parabolic system using two types of receivers.

Description	PTC system with copper receiver	PTC system with commercial receiver
Collector length l_a	2.440 m	2.000 m
Collector area	3.001 m ²	2.460 m ²
Aperture area	2.616 m ²	2.144 m ²
Rim angle ϕ_r	90 °	90 °
Focal distance f	0.268 m	0.268 m
Receiver diameter (External) D_{oa}	15.0 mm	38.0mm
Receiver diameter (Internal) D_{ia}	13.4 mm	-
Collector width w_a	1.072 m	1.072 m
Concentration ratio C	22.7	9.0
Absorber absorptivity α_a	0.96	0.94
Absorber emissivity ϵ_a	0.52	0.06
Mylar reflectance, ρ	0.97	0.97
Glass envelope transmittance τ_g	-	0.95
Mode of tracking	Manual	Manual

A polytetrafluoroethylene (PTFE) inline flowmeter was connected between the tap (water supply) and the inlet to the receiver pipe to regulate and monitor the flowrate during the experiment. Two Xplorer GLX data loggers were used to record the inlet and outlet water temperatures as shown in Fig. 1. This was done at time intervals of 1 minute between 0900 hours and 1600 hours on several days while tracking the movement of the sun by manually rotating the system to remain in focus. The flow rate of the water was varied to investigate its influence on the output temperature and thermal efficiency of the system. The ambient temperature, wind speed and global irradiation values for the specific days were obtained from the Mahalapye meteorological weather station, 70 km away. In another set of experiments, the copper tube receiver was replaced by a commercial receiver purchased from SUNDA solar (China). The key features of the two systems are summarized in Table 1.

III. THEORETICAL BACKGROUND

The optical efficiency of the system is the ratio of the energy absorbed by the receiver to that incident on the aperture. It is dependent on the system’s optical properties such as the reflectance of the concentrator, transmittance of the glass envelope of the receiver, absorption of the receiver’s surface, intercept factor, concentrator’s geometry and construction defect errors. The optical efficiency of a PTC system is given by [7]

$$\eta_o = (\rho_a \tau_g \alpha_r \gamma) K(\theta_i) X_{END} \quad (2)$$

where ρ_a is the collector reflectivity, τ_g is the glass transmittance, α_r is the receiver absorptivity, γ is the intercept factor, $K(\theta_i)$ the incidence angle modifier, θ_i is the angle of incidence in degrees and X_{END} is the end error losses.

Incidence angle modifier $K(\theta_i)$ is the ratio between the optical efficiency at a given incident angle and the efficiency at an incident angle of zero. Assuming a maximum incidence angle of 15 ° (equivalent to one hour of the sun’s motion), the incidence angle modifier as per the LS-2 collector is given by [8]

$$K(\theta_i) = \cos \theta_i + 0.000884(\theta_i) + 0.00005369(\theta_i^2) \quad (3)$$

The end loss error X_{END} for a parabolic trough collector refers to losses occurring as a result of the position of the sun when the incidence angle is not equal to zero. Part of the length of the receiver is not illuminated at incident angles more or less than zero. Fig. 2 shows a schematic diagram on the occurrence of the end losses.

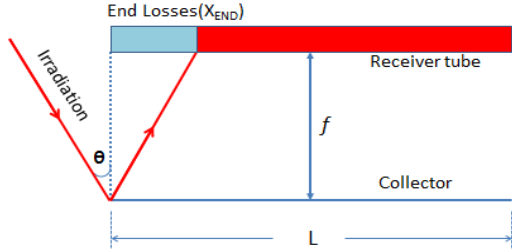


Fig. 2 The end loss effect on a parabolic trough collector

The amount of the loss in irradiation due to the effect is given by [8]

$$X_{END} = 1 - \frac{f}{L} \tan(\theta) \quad (4)$$

The instantaneous thermal efficiency is the useful heat gain Q_u supplied per unit area, A_a per the incident direct irradiation, G_b [9]. It is thus given by

$$\eta_{th} = \frac{\dot{m}c_p(T_o - T_i)}{G_b A_a} \quad (5)$$

where \dot{m} is the mass flow rate of the fluid, c_p is the specific heat capacity of the fluid, and T_o and T_i are the fluid outlet and inlet temperatures respectively. The useful heat absorbed by the receiver tube, Q_u is equivalent to $\dot{m}c_p(T_o - T_i)$. It can also be presented according to thermal and optical heat losses as [9]

$$Q_u = \eta_o G_b A_a - U_L(T_r - T_a)A_r \quad (6)$$

where η_o is the optical efficiency of the system, U_L is the heat loss coefficient, T_r is the receiver temperature, T_a is the ambient temperature, while A_r is the receiver surface area .

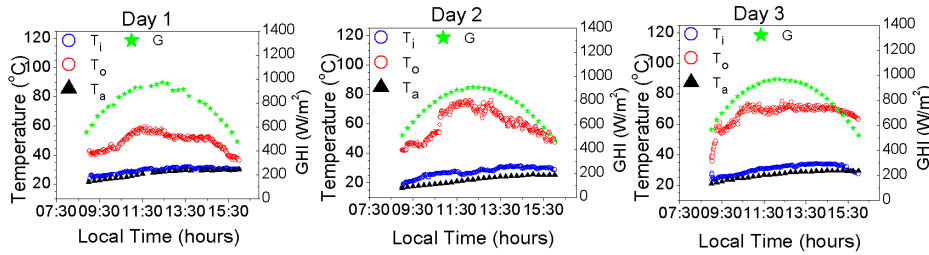


Fig. 3 The inlet, outlet and ambient temperatures and GHI as a function of time for the PTC prototype using coated copper pipe receiver on three different days

The thermal efficiency η_{th} for a concentrating system operating under steady state condition as stipulated by the ASHRAE 1986 [10] is obtained by incorporating Eq. (6) into Eq. (5)

$$\eta_{th} = F_R \eta_o - \frac{F_R U_L}{c} \left(\frac{T_i - T_a}{G_b} \right) \quad (7)$$

Carnot efficiency is the ratio of the work done by a heat engine to the heat drawn out of the high temperature reservoir of the engine. The thermodynamic efficiency limit for a PTC system depends on the fluid inlet temperature (cold reservoir) and the fluid outlet temperature (hot reservoir) as shown in Eq. (8). Therefore the thermal efficiency of a PTC is always equal or less than the Carnot efficiency

$$\eta_c = 1 - \frac{T_i}{T_o} \quad (8)$$

IV. RESULTS AND DISCUSSIONS

A. Optical efficiency

Using parameters in Table 1, the optical efficiencies for the coated copper tube and the commercial receivers were calculated as 76.75 % and 80.34 %, respectively. The intercept factors (γ) for the coated copper tube and the commercial tube were determined as 0.876 and 0.996, respectively by using the approach of Gee et al which is based on the Gaussian approximation [11].

B. Thermal efficiency of the coated copper tube receiver

The water inlet (T_i) and outlet (T_o) temperatures were measured at intervals of 1 minute each day from 0900 hours to 1600 hours. Ambient temperature (T_a) and the global horizontal irradiation (GHI) were obtained from meteorological data provided by the Mahalapye station, 70 km away. The T_i , T_o , T_a and GHI as a function of time for three different days are shown in Fig. 3.

The values of the Carnot efficiency η_c given as calculated from Eq. (8) are shown in Fig. 4 for the three days. The average Carnot efficiency η_o for day one was 38.5 % with maximum values of 50.3 % obtained at 1115 hours. The efficiency dropped gradually to 16.5 % at 1600 hours due to a decrease in the GHI. On day two, the efficiency reached a maximum of 64.8 % at 1145 hours, with an average of 53.6 %. The efficiency then dropped to a minimum of 39.9 % at 1600 hours. Day three showed a much higher average Carnot efficiency of 54.1 % with the highest value of 60.4 % achieved at 1045 hours then decreasing by an average of about 6.4 % and remaining constant at 54.0 %. This shows the highest thermal efficiency that can be reached by the PTC for conditions on those particular days.

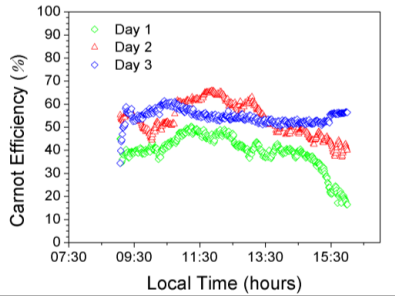


Fig. 4 Carnot efficiency of the PTC prototype when using a coated copper pipe receiver for three different days

When the instantaneous thermal efficiency η_{th} , calculated from Eq. (5) is plotted against the loss in temperature difference $(T_i - T_a)/G_b$, a straight line is obtained if the heat loss coefficient U_L is kept constant. The vertical intercept represents $F_R \eta_o$ while the gradient of the graph is equivalent to $U_L F_R / C$. Fig. 5 shows the thermal efficiency for the three different days using a coated copper pipe of external diameter 15.0 mm.

The thermal efficiency was calculated using values obtained between 1130 hours and 1330 hours where the GHI was at the highest. For this work, the GHI was used to calculate the efficiency because of lack of a Pyrheliometer to measure DNI directly on sight. It is worth noting that the efficiencies obtained therefore gives the lower limit because the GHI value used is greater than the actual DNI absorbed by the system's receiver.

The line of best fit through the plotted data for day one in Fig. 5 could be described by Eq. (9)

$$\eta_{th} = 0.1490 - 2.009 \left(\frac{T_i - T_a}{G} \right) \quad (9)$$

From Eq. (9), we have $F_R \eta_o = 0.1490$ and $F_R U_L / C = -2.009 \text{ W/}^\circ\text{Cm}^2$. Because the geometric concentration, C is 22.7, $F_R U_L$ becomes $-45.60 \text{ W/}^\circ\text{Cm}^2$, according to Eq. (7). From Eq. (2), the optical efficiency of the system $\eta_o = 76.8 \%$, thus resulting in a heat removal factor $F_R = 0.194$. This in turn gives

an overall heat loss coefficient U_L of $-235 \text{ W/}^\circ\text{Cm}^2$. The negative sign shows that heat is given out of the system. The average thermal efficiency calculated using Eq. (5) amounted to 14.96 % and compares well with the value 14.90 % obtained using Eq. (9).

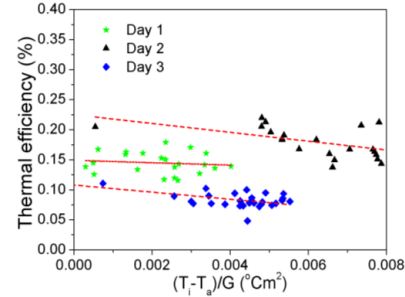


Fig. 5 Thermal efficiency of the PTC using the coated copper tube as a receiver on three different days

For day two the thermal efficiency shown in Fig. 5 is given by the expression

$$\eta_{th} = 0.2251 - 7.362 \left(\frac{T_i - T_a}{G} \right) \quad (10)$$

Eq. (10) gives $F_R \eta_o = 0.2251$ and $F_R U_L / C = -7.362 \text{ W/}^\circ\text{Cm}^2$. When the value of C is substituted, $F_R U_L$ becomes $-167.12 \text{ W/}^\circ\text{Cm}^2$. From Eq. (2), the optical efficiency of the system $\eta_o = 76.8 \%$, resulting in a heat removal factor of $F_R = 0.293$. This in turn gives an overall heat loss coefficient U_L of $-570.38 \text{ W/}^\circ\text{Cm}^2$. The average thermal efficiency calculated using Eq. (5) was 17.48 % and compares well with the value of 22.51 % obtained using Eq. (10).

Thermal efficiency for day three is represented by the expression

$$\eta_{th} = 0.1129 - 6.919 \left(\frac{T_i - T_a}{G} \right) \quad (11)$$

which gives $F_R \eta_o = 0.1129$ and $F_R U_L / C = -6.919 \text{ W/}^\circ\text{Cm}^2$. From Eq. (2), the optical efficiency of the system remain $\eta_o = 76.8 \%$, giving a heat removal factor $F_R = 0.147$ and hence the overall heat loss coefficient U_L becomes $-1068.62 \text{ W/}^\circ\text{Cm}^2$. The average thermal efficiency calculated using Eq. (5) was 7.65 % and compares well with the value of 8.24 % obtained using Eq. (11). The results of the performance of the coated copper receiver system on the three days are summarized in Table 2.

The wind speed on day 1 and day 3 were the same but according to Eq. (5) the thermal efficiency on day 1 was twice that of day 3 because the mass flow rate for day 1 was thrice that of day 3 despite the larger temperature change on day 3. The thermal efficiency was highest on day two probably because of the higher change in temperature and lower wind speed coupled with the relatively lower GHI value. The influence of the wind speed on the outlet temperature and hence

thermal efficiency can be seen for day 2 when compared to the other days.

Table 2 A summary of the performance parameters for the coated copper receiver system for the three days.

Day	1	2	3
GHI (W/m ²)	923.8	895.4	953.5
T _i (°C)	30.6	27.6	32.3
T _a (°C)	28.6	22.7	28.0
T _o (°C)	54.6	71.2	70.3
ΔT (°C)	24.0	43.6	38.0
Mass Flow (kg/s)	0.0036	0.0026	0.0012
Carnot Efficiency η _c (%)	43.91	61.06	54.06
Thermal Efficiency η _{th} (%)	14.96	19.60	7.65
Optical Efficiency η _o (%)	76.8	76.8	76.8
Wind speed (m/s)	4.4	2.8	4.4

C. Thermal efficiency of the commercial receiver

The inlet, outlet and ambient temperatures as well as the GHI obtained with the 2.00 m long commercial receiver having glass envelope insulation are shown in Fig. 6.

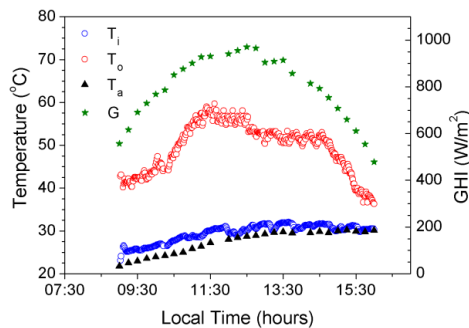


Fig. 6 The inlet, outlet, ambient temperatures and GHI as a function of local time for the PTC with a commercial receiver

On this day, the mass flow rate was set at 0.0036 kg/s. The highest temperature of the water at the outlet was about 60 °C, which is slightly higher than 54.6 °C obtained with the coated copper receiver on a day with a similar mass flow rate.

Carnot and thermal efficiency of the system using the commercial receiver are shown in Fig. 7 as a function of the local time and $(T_i - T_a)/G$, respectively. The average Carnot efficiency for the commercial receiver was found to be 45.67 % with the maximum obtained as 53.26 % at 1230 hours and the lowest being 22.0 % at 1545 hours. The thermal efficiency of the commercial receiver can be described by a linear fit given by

$$\eta_{th} = 0.2776 - 18.242 \left(\frac{T_i - T_a}{G} \right) \quad (12)$$

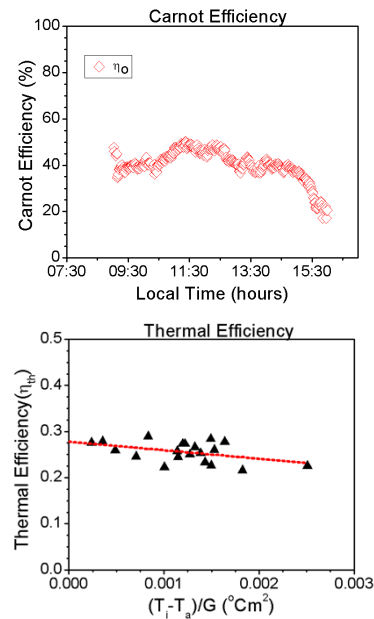


Fig. 7 a) Carnot and b) thermal efficiency of the commercial receiver

This gives $F_R \eta_o = 0.2776$ and $F_R U_L / C = - 18.242$ W/°Cm². Substituting for the concentration ratio, $C = 9.0$ gives the value of $F_R U_L$ as $- 164.178$ W/°Cm². The optical efficiency for the commercial receiver was computed using Eq. (5) to be 80.3 %, thus resulting in a heat removal factor $F_R = 0.346$. The overall heat loss coefficient is thus equivalent to $- 474.50$ W/(°Cm²). The average thermal efficiency calculated using Eq. (5) was 26.61 % and compares well to the value of 29.24 % obtained using Eq. (12). The performance parameters obtained for the commercial receiver have been summarized in Table 3.

The performance of the commercial receiver and that of the coated copper tube receiver in this work cannot be compared directly due to the difference in their concentration ratios of 9.0 and 22.7, respectively. The output temperatures achieved in this work show that the PTC can be used for application in industrial process heating especially in food industry where the temperatures needed lie in the range of 60 - 180 degrees [12]. The outlet temperatures from this work are higher than 47.3 °C reported by Macedo-Valencia et al for a PTC of length 0.98 m, width 0.58 m, a concentration ratio 67.17 and a rim angle of 90 ° [13]. Jaramillo et al [14] and Rizwan et al [15] reported higher outlet temperatures of 107.5 °C and 106 °C, with input temperatures of 25 °C and 30 °C respectively. The mass flow rates used by Jaramillo et al and Rizwan et al were 0.000694 kg/s and 0.0003400 kg/s, respectively while for this work the flow rates were relatively higher at 0.0012 kg/s

up to 0.0036 kg/s. the performance of the PTC prototype reported in this work, is therefore comparable to others tested elsewhere.

Table 3 Measured parameters and calculated efficiencies for the commercial receiver

GHI (W/m ²)	1050.2
T _i (°C)	30.0
T _a (°C)	36.9
T _o (°C)	77.8
ΔT (°C)	47.8
Mass Flow (kg/s)	0.0036
Carnot Efficiency η _c (%)	51.10
Thermal Efficiency η _m (%)	26.61
Optical Efficiency η _o (%)	80.3
Wind speed (m/s)	2.8

V. CONCLUSION

A PTC prototype was constructed and tested under terrestrial conditions of Botswana for the first time at Botswana International University of Science and Technology. The results show very high optical efficiencies close to 80 % although the thermal efficiencies were below 50 % for the coated copper tube. The highest thermal efficiency was achieved on day two where the wind speed was the lowest at 2.8 m/s. It is clear that the wind has a strong effect on the thermal efficiency of the PTC. The performance of the system with a commercial receiver was different because of the different (lower) concentration ratio; therefore we cannot compare the performance of the two systems. With these results, the performance of the prototype can be improved by improving on the concentration ratio of the commercial system.

VI. ACKNOWLEDGMENT

This work was supported and financed by the Botswana International University of Science and Technology (BIUST).

VII. REFERENCES

- [1] J. Sawin and E. Martinot, "Renewable Energy World," The World's #1 Renewable Energy Network for News, Information, and Companies, 29 September 2011. [Online]. Available: <http://www.renewableenergyworld.com>. [Accessed 19 March 2019].
- [2] D. Gielen, "Cost analysis series; concentrating solar power vol 1: power sectors, issue 2/5," IRENA, Europe, 2012.
- [3] S. Kraemer, "Renewable Energy World," The World's #1 Renewable Energy Network for News, Information, and Companies., 29 March 2016. [Online]. Available: <http://www.renewableenergyworld.com>. [Accessed 28 April 2019].
- [4] IRENA, "CSP Plaza, tracking the world csp industry," cspplaza, 29 January 2016. [Online]. Available: <http://en.cspplaza.com>. [Accessed 18 February 2019].
- [5] Wiston and Strawn, "LEXOLOGY," Globe Business Media Group, 10 August 2016. [Online]. Available: <http://www.lexology.com>. [Accessed 24 April 2019].
- [6] B. Benza, "MmegiOnline," 02 June 2016. [Online]. Available: <http://www.mmegi.bw>. [Accessed 25 April 2019].
- [7] A. V. Arasu and T. Sornakumar, "Performance characteristics of Parabolic Trough Solar collector system for hot water generation," *International Energy Journal*, vol. 7, no. 2, pp. 137-145, 2006.
- [8] V. E. Dudley, G. Kolb, A. R. Mahoney, T. R. Mancini, C. W. Matthews, M. Sloan and D. Kearney, "Test results: SEG ls-2 solar collector," Sandia National Laboratories, Albuquerque, New Mexico, 1994.
- [9] S. Kalogirou, "Parabolic triugh collector system for low temperature steam generation: Design and performance characteristics," *Applied Energy*, vol. 55, no. 1, pp. 1-19, 1996.
- [10] S. 9. ASHRAE, "Method of testing to determine the thermal performance of solar collectors.," American society of heating, refrigeration and air-conditioning engineers, Atlanta, GA, 1986.
- [11] R. Gee, R. Brost, G. Zhu and G. Jorgensen, "ReflectechSolar," 2010. [Online]. Available: <http://www.reflectechsolar.com>. [Accessed 19 February 2019].
- [12] A. G. Bhawe, "Industrial process heat applications of solar energy," *International Journal of Modern Engineering Research*, vol. 2, no. 5, pp. 3800-3802, 2012.
- [13] J. Macedo-Valencia, J. Ramirez-Avila, R. Acosta, O. A. Jaramillo and J. O. Aguillar, "Design, construction and evaluation of parabolic trough collector as demonstrative prototype," *Energy procedia*, vol. 57, pp. 989-998, 2014.
- [14] O. A. Jaramillo, E. Veneges-Reyes, J. O. Aguilar, R. Castrejon-Garcia and F. Sosa-Montemayor, "Parabolic trough concentrators for low enthalpy processes," *Renewable Energy*, vol. 60, pp. 529-539, 2013.
- [15] M. Rizwan, A. R. Junaid, M. Suleman and M. A. Hussain, "Experimental verification and analysis of solar parabolic

BIUST Research and Innovation Symposium 2019 (RDAIS 2019)
Botswana International University of Science and Technology
Palapye, Botswana, 4 - 7 June 2019



ISSN: 2521-2292

collector for water desalination," *International Journal of
engineering research*, vol. 3, no. 10, pp. 558-593, 2014.